



Missouri University of Science and Technology
Scholars' Mine

International Specialty Conference on Cold-Formed Steel Structures

(2014) - 22nd International Specialty Conference on Cold-Formed Steel Structures

Nov 6th, 12:00 AM - 12:00 AM

Development of a Novel Pinned Connection for Cold-Formed Steel Trusses

Chris D. Mathieson

G. Charles Clifton

James B. P. Lim

Follow this and additional works at: <https://scholarsmine.mst.edu/isccss>

 Part of the [Structural Engineering Commons](#)

Recommended Citation

Mathieson, Chris D.; Clifton, G. Charles; and Lim, James B. P., "Development of a Novel Pinned Connection for Cold-Formed Steel Trusses" (2014). *International Specialty Conference on Cold-Formed Steel Structures*. 5.

<https://scholarsmine.mst.edu/isccss/22iccfss/session10/5>

This Article - Conference proceedings is brought to you for free and open access by Scholars' Mine. It has been accepted for inclusion in International Specialty Conference on Cold-Formed Steel Structures by an authorized administrator of Scholars' Mine. This work is protected by U. S. Copyright Law. Unauthorized use including reproduction for redistribution requires the permission of the copyright holder. For more information, please contact scholarsmine@mst.edu.

Development of a Novel Pinned Connection for Cold-Formed Steel Trusses

Chris D. Mathieson¹, G. Charles Clifton², James B.P. Lim³

Abstract

Cold-formed steel trusses are a popular form of construction for light-weight buildings, particularly portal frame structures, for which spans up to 25m are increasingly common. In these long span trusses, providing high strength connections with sufficient elastic stiffness is a current limitation to developing cost-effective solutions. A novel pin-jointed truss connection named the Howick Rivet Connector (HRC) has been tested, firstly in a T-joint arrangement, then in a truss assemblage to determine its reliable strength and stiffness. Results showed that the HRC performs similarly to a bolted connection in terms of failure modes observed and loads reached. Additionally, the process of installing the HRC creates a bearing fit, eliminating slip due to tolerances. The elastic stiffness and proportionality limit of trusses with HRCs installed was shown to be appreciably greater than similarly dimensioned conventional screwed systems. Finite element (FE) models of both T-joints and trusses tested showed good agreement with experimental results, particularly in the transition from elastic to inelastic behaviour. The peak loads predicted from the FE models were however not accurately determined. To better predict this, it is recommended that the HRC forming and installation process be modelled to capture geometric irregularities and inelastic distributions which were idealised.

¹ Master of Engineering Student, 2013, Department of Civil and Environmental Engineering, The University of Auckland, New Zealand.

² Associate Professor, Department of Civil and Environmental Engineering, The University of Auckland, New Zealand.

³ Senior Lecturer, Department of Civil and Environmental Engineering, The University of Auckland, New Zealand.

Introduction

Cold-formed steel (CFS) is commonly used to construct light weight trusses which rely on pin-jointed connections to transmit tension and compression forces between the chord and web members in shear. The use of CFS in structural applications has traditionally been limited to secondary elements such as roof purlins, wall studs and floor joists, however CFS is increasingly being used as the frames in portal structures (Bayan, Sariffuddin et al. 2010). The thickness of CFS structural members typically range from 0.95mm to 3.0mm, while sections as thin as 0.55mm are becoming more common. The typical yield stress of CFS ranges from 250N/mm^2 to 550N/mm^2 depending on the degree of rolling and heat treatment.

Screws are the most common method of providing a pinned or shear connection in CFS trusses and can also be used to form moment connections in portal frames. The main limitation of screws are their relatively low strength in shear which often leads to several screws being required to provide adequate strength at a connection. This increases installation time and can create spacing limitations. In the case of moment connections, the cost and buildability make it uneconomical to construct portal frames greater than 25m in span.

Bolts are commonly used in CFS structures where high strength is required in a connection and screws or other methods cannot provide this. One of the main limitation of using bolts arises from the pre-drilling of the bolt holes. When initially load in shear, a bolted connection will undergo slip due to these tolerances which causes extension in shear connections and a reduction in stiffness for moment connections (Lim, Nethercot 2004).

A novel pin-jointed connection named the Howick Rivet Connector (HRC) has been developed as an alternative to both screw and bolted connections in CFS trusses (Figure 1). The HRC provides a pinned connection between lipped channel sections through their flanges by clamping them between an inner and outer swage. The intended application of the HRC is to connect the chord and lattice members of trusses used in floors, roofs and portal frames. Knee and apex connections used in portal frames comprising truss sections can also be fabricated using an array of HRCs with the aid of gusset plates. It should be noted that the process of creating the outer swages forces a bearing fit between the rivet shank (portion of HRC between the inner and outer swage) and the holes of the connected members because the shank undergoes a small degree of outward flaring.

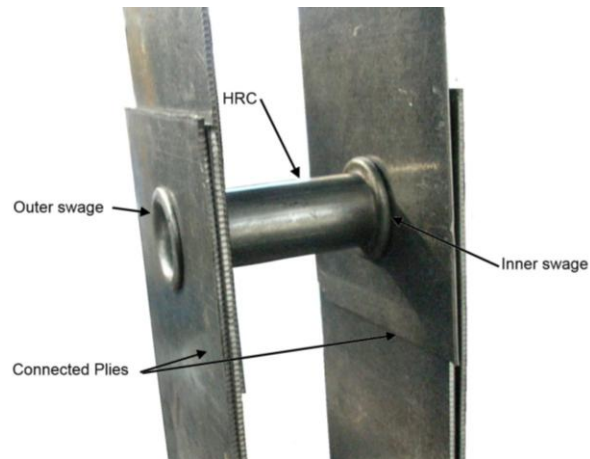


Figure 1: Howick Rivet Connector

The purpose of this paper is to present preliminary tests which were performed on a series of T-joint and short truss specimens to determine the reliable strength and stiffness of connections comprising a HRC. The trusses were tested to determine how the connector performs in a realistic assembly. Finite element (FE) models of the T-joint and one of the truss tests were also created to expand the understanding of the system and allow investigation into different combinations of variables in future research without relying solely on experimental testing.

T-Joint Specimens

The rig used for testing the HRC T-joints is shown in Figure 2. The vertical member of the T-joint was bolted to plates connected to the top of a 100kN Instron frame which allows free rotation about all axes. The horizontal member was clamped to the crosshead beam of the Instron which pulled down on the horizontal plates at a rate of between 0.6mm and 0.8mm per second. Two portal gauges were set up on either side of the connection to mitigate errors due to tilting during testing. The lips of the horizontal member were cut to allow the same sized vertical member through and the corners of the vertical member inside the T-joint specimen were chamfered at 45 degrees so that it can be oriented diagonally in a truss assembly.

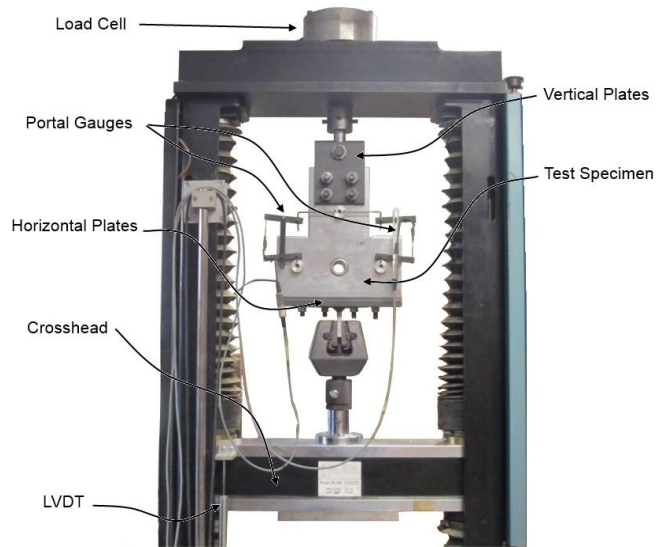


Figure 2: T-Joint Specimen Test Setup

Two member sizes (Figure 3 and Figure 4) were tested with a corresponding combination of member thicknesses and rivet sizes. The size and thickness of each element tested is presented in Table 1 along with their respective yield and tensile strengths. The material strengths were determined according to ISO 6892-1:2009 (2009) using reduced specimens and are only shown for the direction parallel to rolling. The material properties of the HRC were determined from the initial blank tube. Modifications to the standard HRC such as adding washers and providing steel inserts were also tested, however these are not presented in this paper.

Table 1: Section and Material Properties

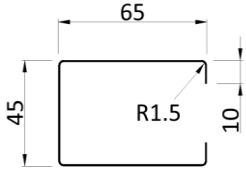
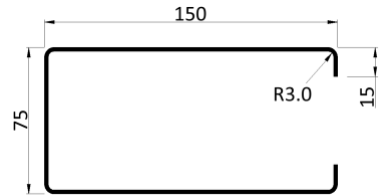
Section Tested (mm)	Member Thickness (mm)	Yield Stress (N/mm ²)	Ultimate Stress (N/mm ²)
	0.75	630	650
	0.95	660	660
	1.15	600	610
	Rivet Sizes (mm)		
	12.7x0.95	390	402
	12.7x1.55	430	437
	15.9x1.15	410	422

Figure 3: 65x45mm Lipped C-Section



Member Thickness (mm)	Yield Stress (N/mm ²)	Ultimate Stress (N/mm ²)
1.6	560	580
1.85	280	390
2.4	320	400
3.0	390	520
Rivet Size (mm)		
31.8x1.85	370	381

Figure 4: 150x75mm Lipped C-Section

Results

The results from testing revealed two modes of failure which were shear failure of the HRC and bearing failure of the connecting plies. The results of all T-joint tests are outlined in Table 2 which includes the average peak load, standard deviation and failure modes. Each test was conducted three times.

Table 2: Results of T-Joint Tests

Rivet Size	Member Thickness (mm)	Average Peak Load (kN)	Standard Deviation (kN)	Failure Mode
12.7x0.95mm	0.75	12.31	1.12	Bearing
	0.95	15.76	0.74	Shear
	1.15	15.81	0.60	Shear
12.7x1.55mm	0.75	10.81	0.17	Bearing
	0.95	16.54	0.68	Bearing
	1.15	20.68	0.44	Bearing
15.9x1.15mm	0.75	13.34	0.20	Bearing
	0.95	17.98	0.56	Bearing
	1.15	21.90	0.63	Bearing
31.8x1.85mm	1.6	72.58	0.77	Bearing/Shear
	1.85	49.35	4.33	Bearing
	2.5	74.50	0.6	Shear
	3.0	76.12	1.2	Shear

A plot of typical loading to failure for a T-joint which underwent bearing failure is shown in Figure 5 with stages defined and explained as follows:

1. **Elastic Range** - the HRC and connected plies behave elastically.

2. **Onset of Bearing Failure** - the plies that are bearing on the HRC become increasingly unstable as the bearing surface becomes inelastic and the rivet hole begins to extend.
3. **Peak Load** - the highest load reached.
4. **Buckling** - the failed member buckles significantly out-of-plane.
5. **Ply Bearing and Work Hardening** - The buckled plies stop deforming out-of-plane and begin to utilise the added bearing area gained by folding onto the swages while work hardening.
6. **Inelastic Redistribution** - as the ply materials continue to work harden, redistribution of stresses around the rivet hole occurs.
7. **Ultimate Failure** - one or both sets of plies rupture.

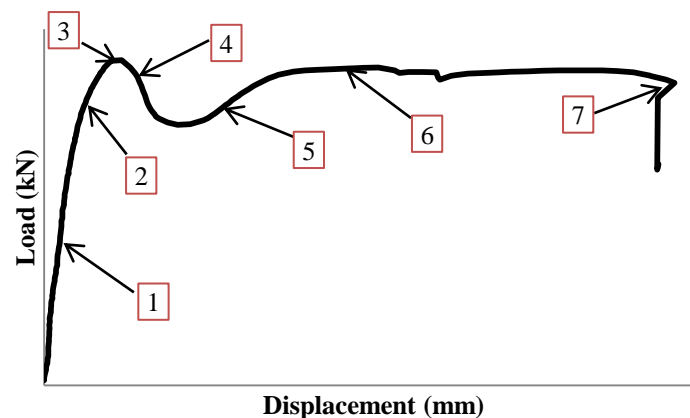


Figure 5: Typical T-joint Which Underwent Bearing Failure

An example of a T-joint specimen which failed in bearing is shown in Figure 6. It was observed in most tests which failed in bearing that the flanges of the vertical member folded inwards. The buckling and folding of plies is typical of bearing failure where the plies act to align themselves with the applied axial forces. Adding washers to both sides of the HRC significantly increases the bearing capacity of HRC connection as out-of-plane buckling is largely suppressed, however this set of testing is not specifically presented in this paper.

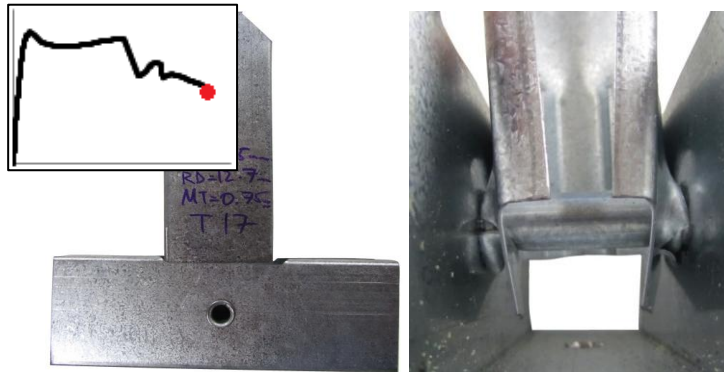


Figure 6: Example of Bearing Failure (0.75mm Member; 12.7x0.95mm HRC)

A plot of typical loading to failure for a T-joint which underwent shear failure is shown in Figure 7 with stages defined and explained as follows:

1. **Elastic Range** - the HRC and connected plies behave elastically.
2. **Rivet Softening** - the HRC starts to become inelastic and form plastic hinges.
3. **Rivet Squashing** - the HRC continues to squash into an oval shape with plastic hinges fully formed.
4. **Ultimate Failure** - the HRC ruptures.

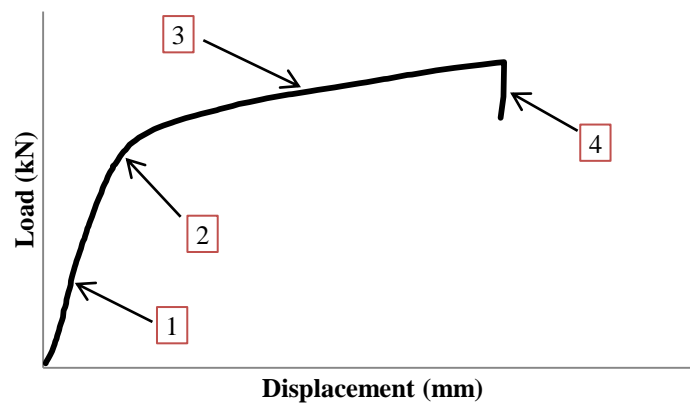


Figure 7: Typical T-joint Test Which Underwent Shear Failure

An example of a T-joint specimen which failed in shear is shown in Figure 8. The onset of yielding occurred along the centreline of the rivet orthogonal to the direction of loading. This area of the rivet has the greatest volume of material which is oriented parallel to the direction of loading. Once plastic hinges develop, this area is also where there is the greatest curvature which creates large strains.

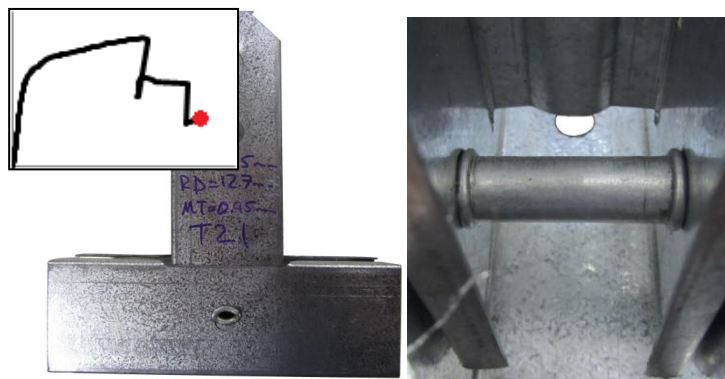


Figure 8: Example of Shear Failure (0.95mm Member; 12.7x0.95mm HRC)

The two modes of failure observed are similar to bolted connections in CFS members. Provisions in the Australian/New Zealand Standard (AS/NZS) (2005) for predicting bearing failure have been shown to be underconservative in the case of CFS truss connections where the central member is unrestrained (Yu, Panyanouvong 2013) which is the same case as is presented in this paper. It should be noted that these formulae are equivalent to the North American Specification (2007). A comparison between the T-joint tests which failed in bearing, the AS/NZS provisions and the formulae proposed by Yu (Yu, Panyanouvong 2013) are shown in Figure 9. It can be concluded from this figure that the strength of the HRC in bearing is most consistent with the latter formula. The inner swage of the HRC was found to slightly increase the bearing strength of the connection as it acted to confine the inner plies.

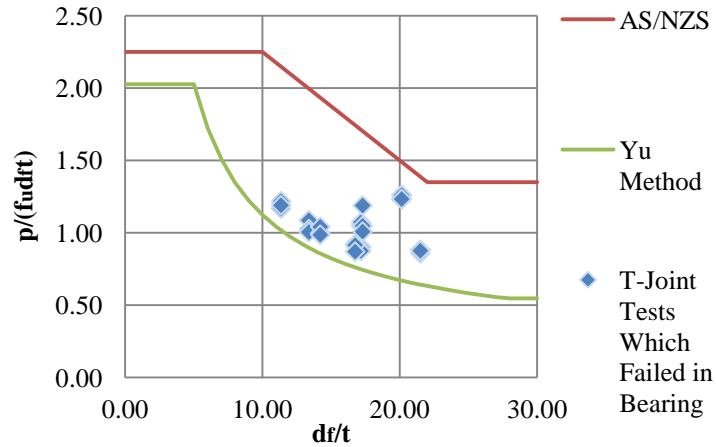


Figure 9: Bearing Failure of T-Tests Compared to Current and Proposed Design Formulae

The strength of the HRC in shear was also shown to be consistent with current code provisions for bolts in shear which imply proportionality between the tensile and shear strength of bolts. Figure 10 shows that the shear strength of the HRC is directly proportional to its cross sectional area multiplied by the ultimate stress.

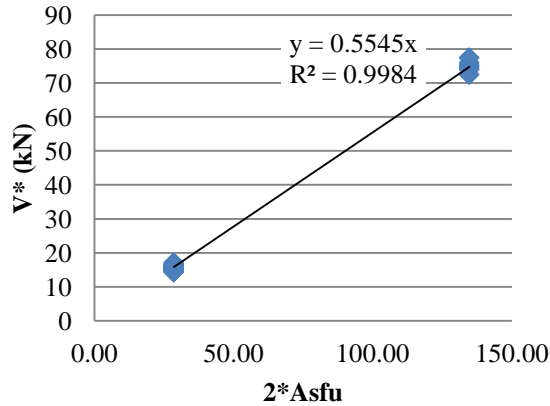


Figure 10: Tensile Capacity of HRC Against Applied Shear Force

Finite Element Model

Finite element (FE) models of a selection of the T-joint tests were created using ABAQUS/Standard v6.12-3 (Simulia 2012) as an attempt to better understand the distribution of stresses and to predict the failure limit states in the connection. Parts were modelled using first order solid elements as these provide a more robust contact solution than second order elements. C3D8R elements were used to model tests which failed in shear and C3D8I elements for tests which failed in bearing. The C3D8I elements perform better in bending than C3D8R (Može, Beg 2014), however they are sensitive to element distortions which can significantly reduce accuracy (Simulia 2012) so were not used for all models. Surface-to-surface contact was used and a plane of symmetry assumed to reduce runtime. An example of one of the T-joint test models is in Figure 11.

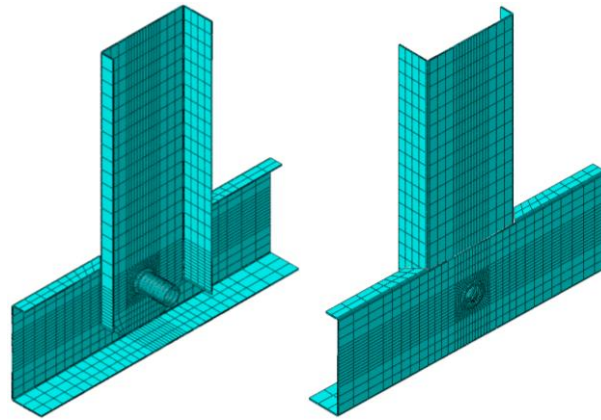


Figure 11: FE model of T-Joint (0.95mm Member; 12.7x0.95mm HRC)

A comparison between the FE results and experimental are shown in Figure 12. The material properties were assumed to be perfectly plastic after the ultimate stress was reached. It can be seen that the FE model displayed a similar loading behaviour to the experimental tests, but eventuated in different peak loads. The under prediction in the peak load for tests which failed in shear was likely due to work hardening during the assembly of the connection which was unaccounted for in the models. The over prediction in peak load for the tests which failed in bearing was attributed to the idealisation of geometric imperfections which did

not allow for initial buckled shapes. It is recommended that the HRC installation process be modelled prior to load application to better simulate the connection.

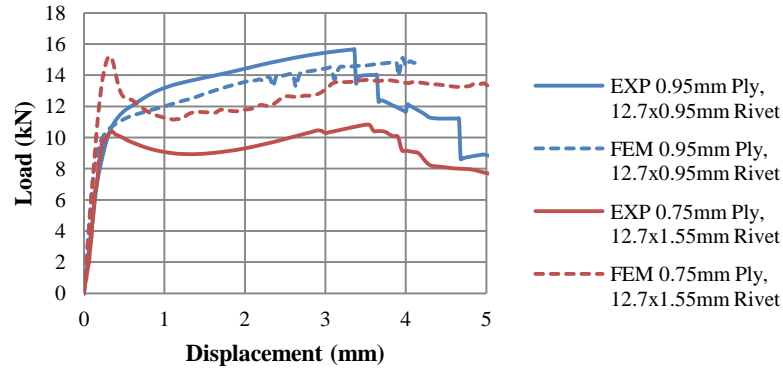


Figure 12: Comparison of T-Joint Experimental and Model Results (EXP = Experimental; FEM = Finite Element Model)

Truss Testing

A series of short span trusses were tested to determine how the HRC performs in a realistic assembly. The typical dimensions of trusses with HRCs is in Figure 13 and the experimental setup is shown in Figure 14. The trusses were supported on rollers to allow rotation of the ends of the specimen. LVDTs were set up underneath the centre of the truss to measure midpoint deflection and also above the left and right supports to ensure deflections are relative to the distance between the top and bottom chords of the truss. The load to the truss was applied via a load spreading beam which was allowed to rotate about the axes perpendicular to the span of the truss onto two bearing pads. These pads were sized to spread the load over an area sufficient to reduce the chance of bearing failure.

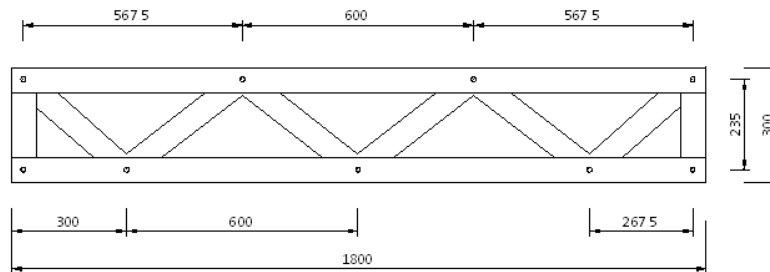


Figure 13: Typical Dimensions of Truss Specimens with HRCs at Connections

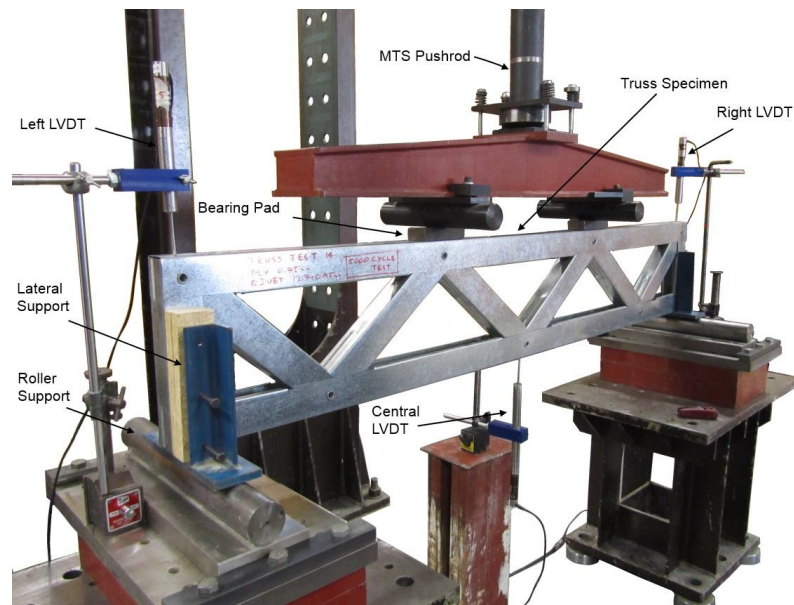


Figure 14: Experimental Test Setup for Truss Testing

Two types of truss were tested using the experimental setup. The first were trusses connected with HRCs using the 65x45mm members 0.75mm and 0.95mm thick, as these resulted in bearing and shear failure modes respectively in the T-joint tests (Figure 15a). The second type of truss tested used 90x40mm members 0.75mm thick (Figure 15 b). The configuration and connections of the trusses with screws are typically used in residential floors and were tested as a comparison to similarly sized trusses with HRCs. Four of each truss with HRCs and two trusses with screw connections were tested.



Figure 15: Truss Connection with HRC (a) and Standard Screws (b)

Results

Similar to the T-joint tests, there were two main failure mechanisms which were bearing and shearing of the HRC. The trusses with screw connections failed in tilting, fracture and pullout. The results for the truss tests are shown in Table 3. It was found that the size of the outer swage directly affected the bearing capacity of the connection which is why there is a large deviation in results for trusses which failed in bearing at the critical connection.

Table 3: Results of Truss Tests

Type of Truss Connection	Member Thickness (mm)	Average Peak Load (kN)	Standard Deviation (kN)	Failure Mode
HRC	0.75	10.78	2.04	Bearing
	0.95	19.68	0.42	Shear
Screws	0.75	10.05	1.44	Screw Fracture/ Pullout

A comparison between typical trusses connected with HRCs 0.75mm and 0.95mm thick and the trusses with screw connections is shown in Figure 16. It can be seen from this plot that the stiffness and proportionality limit of trusses connected with HRCs is appreciably greater than the similarly dimensioned conventional screwed systems.

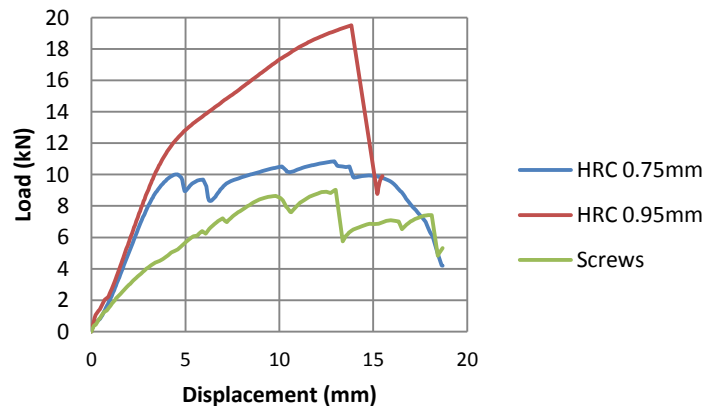


Figure 16: Comparison of Typical Truss Tests

Finite Element Model

A finite element model of the truss with 0.95mm thick members connected with HRCs was made using the same model properties as the T-joint tests (Figure 17). Symmetry could only be achieved along one plane due to overlap of web members. The results from the FE model were agreeable with the experimental testing, especially in the transition from elastic to post-elastic behaviour (Figure 18), however the model failed to converge once the critical connections reached their ultimate yield stress. The plot for the FE model is translated 2.15mm which was proven to be due to slip in the experimental tests.

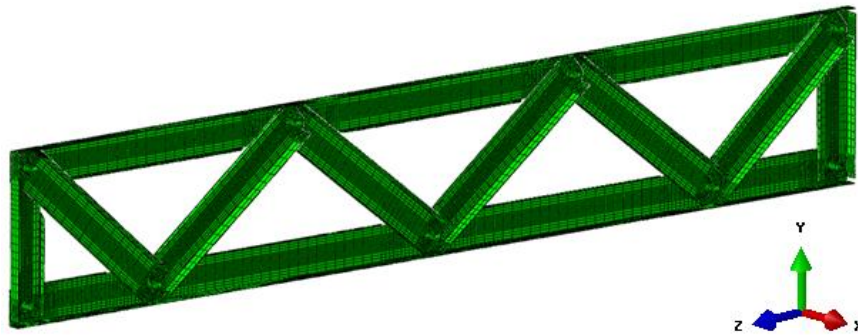


Figure 17: FE Truss Model

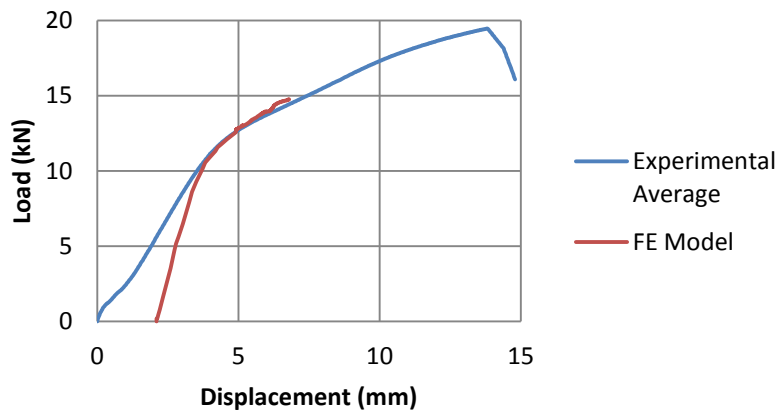


Figure 18: Comparison of Experimental and FE Model Truss Results (FE Results Translated 2.15mm)

Overall Conclusions

A series of T-joint and short span truss tests were conducted on the HRC. These tests showed that the HRC performs similarly to a bolted connection as connections fail in either bearing or shear failure. Trusses connected with HRCs were shown to have a greater elastic stiffness and proportionality limit than similarly sized trusses with eccentric screw connections. FE models of both the T-joint and truss tests showed good agreement with the experimental results, however the peak loads were not accurately captured due to idealisation of the manufacturing process. It is recommended that FE models include this process in future studies.

Acknowledgements

The authors would like to thank Howick Ltd. for providing all test materials and specimens and for funding the project.

References

- AISI. 2007. "North American Specification for the Design of Cold-Formed Steel Structural Members." *2007 Edition*, AISI S100-2007.
- BAYAN, A., SARIFFUDDIN, S. and HANIM, O., 2010. Cold formed steel joints and structures-A review. *International Journal*, **2**(2), pp. 612-625.
- ISO, E., 2009. *6892-1: 2009: Metallic materials-Tensile testing-Part 1: Method of test at room temperature*.
- LIM, J.B.P. and NETHERCOT, D.A., 2004. Stiffness prediction for bolted moment-connections between cold-formed steel members. *Journal of Constructional Steel Research*, **60**(1), pp. 85-107.
- MOŽE, P. and BEG, D., 2014. A complete study of bearing stress in single bolt connections. *Journal of Constructional Steel Research*, **95**(0), pp. 126-140.
- ABAQUS/Standard Version 6.8-2; Abaqus/CAE User's Manual. (2008), Dassault Systèmes Simulia Corp., Providence, RI, USA.
- STANDARDS AUSTRALIA, I.L., 2005. *Cold-formed steel structures*. Sydney, N.S.W. : Standards Australia ; Wellington N.Z. : Standards New Zealand, 2005.
- YU, C. and PANYANOUVONG, M.X., 2013. Bearing strength of cold-formed steel bolted connections with a gap. *Thin-Walled Structures*, **67**(0), pp. 110-115.